

# Capacitive properties of polypyrrole/activated carbon composite

Aleksandra Porjazoska Kujundziski<sup>1</sup>, Dragica Chamovska<sup>2</sup>, Toma Grchev<sup>2</sup>

<sup>1</sup>International Balkan University, Faculty of engineering, Macedonia

<sup>2</sup>Faculty of Technology and Metallurgy, Sts. Cyril & Methodius University, Skopje, Macedonia

## Abstract

Electrochemical synthesis of polypyrrole (PPy) and polypyrrole/activated carbon (PPy/AC) – composite films, with a thickness between 0.5 and 15  $\mu\text{m}$  were performed in a three electrode cell containing 0.1 mol  $\text{dm}^{-3}$  Py, 0.5 mol  $\text{dm}^{-3}$   $\text{NaClO}_4$  dissolved in ACN, and dispersed particles of AC (30 g  $\text{dm}^{-3}$ ). Electrochemical characterization of PPy and PPy/AC composites was performed using cyclic voltammetry (CV) and electrochemical impedance spectroscopy (EIS) techniques. The linear dependences of the capacitance ( $q_c$ ), redox capacitance ( $q_{\text{red}}$ ), and limiting capacitance ( $C_L$ ) of PPy and PPy/AC – composite films on their thickness ( $L$ ), obtained by electrochemical and impedance analysis, indicate a nearly homogeneous distribution of the incorporated AC particles in the composite films (correlation coefficient between 0.991 and 0.998). The significant enhancement of  $q_c$ ,  $q_{\text{red}}$  and  $C_L$  was observed for composite films (for 40 $\pm$ 5%) in respect to that of the “pure” PPy. The decreased values of a volume resistivity in the reduced state of the composite film,  $\rho = 1.3 \times 10^5 \Omega \text{ cm}$  (for  $L = 7.5 \mu\text{m}$ ), for two orders of magnitude, compared to that of PPy – film with the same thickness,  $\rho \approx 10^8 \Omega \text{ cm}$ , were also noticed.

**Keywords:** conducting polymers, composites, cyclic voltammetry, electrochemical impedance spectroscopy (EIS), electrical equivalent circuits (EECs).

Available online at the Journal website: <http://www.ache.org.rs/HI/>

Electrochemical capacitors (ECs) as power devices, with the possibility of completely charging or discharging in seconds, have an important role in complementing or substituting conventional batteries [1]. Depending on the charge storage mechanism, as well as the active material used, two types of ECs can be distinguished.

The first type is a double layer kind of capacitance that uses carbon-based active materials with a relatively high electronic conductivity, electrochemical stability and acceptable cost [2,3]. The power and energy-storage capabilities of these devices are closely linked to the physical and chemical characteristics of carbon electrodes. For example increases in specific surface area obtained through the activation of carbon, generally lead to an increased capacitance [3–5].

A second group of ECs, known as pseudocapacitors or redox supercapacitors, uses fast and reversible surface or near-surface reactions, Faradaic chemical processes. Transition metal oxides, as well as electrically conducting polymers (polyaniline, polypyrrole, polythiophene and their derivatives), have been tested in EC applications as pseudocapacitance materials [6].

In the case of the conducting polymer materials, it becomes somewhat difficult to distinguish whether the charging process is to be considered as the double layer

type or a redox pseudocapacitance nature [1]. However, the capacitance developed on a conducting polymer holds a Faradaic origin with process of chemical/ /electronic changes like formation or removal of radical cation or radical anion centers indicating a pseudocapacitance character [6–9].

Among the conducting polymers known to date, ones based upon polypyrrole (PPy) have attracted great attention because of their excellent environmental stability, tuned electrical conductivity and biocompatibility [10,11], and potential technical application in various fields, such as in electronic and electrochromic devices [8], electrode material in supercapacitors [6,9], sensors [12], light-weight batteries [13], membrane separation [14], corrosion protection [15–17] or substrates for tissue engineering [10,11].

When used as bulk materials, conducting polymers suffer from a limited stability during cycling that reduces the initial performance [18]. The mechanical properties and electrochemical stability might be improved *via* preparation of graft and block copolymers [19], as well as systems comprising two electrochemically active components [3,6], one with a double layer capacitance, (carbon fibers or carbon black), and the other, with a pseudo-capacitance (Faradaic) features (electroconducting polymers, such as PPy) [20,21].

Thus, Kim *et al.* [3] prepared PPy/vapor grown carbon fibers/AC (PPy/VGCF/AC) composites characterized by both, pseudo and electric double layer capacitance. As observed by cyclic voltammetry, the specific capacitances of composites in 6 mol  $\text{dm}^{-3}$  KOH

Polymers

SCIENTIFIC PAPER

UDC 544.6:54–126:543.42

Hem. Ind. 68 (6) 709–719 (2014)

doi: 10.2298/HEMIND140305063P

Correspondence: T. Grchev, Faculty of Technology and Metallurgy, Sts. Cyril & Methodius University, Skopje, Macedonia.

E-mail: dragica@tmf.ukim.edu.mk

Paper received: 5 March, 2014

Paper accepted: 27 August, 2014

raises from  $\sim 165 \text{ F g}^{-1}$  for 5 wt.% AC, to  $\sim 338 \text{ F g}^{-1}$  for 60 wt.% AC in electrodes of 2 nm-thick PPy film deposited on a highly conductive carbon fiber.

One of the techniques of capacitance enhancement and supercapacitors life-cycles, nanocomposites based on electronically conductive polymers and carbon nanotubes [4] and / or conductive carbon powder have been prepared [5]. It was shown [4] that the specific capacitance of such systems increased with both, the nanotubes amount, and the PPy content in the composites.

Despite the advantages of carbon nanotubes concerning their mechanical, thermal, electrical properties, as well as their big specific area, very complex techniques for their synthesis, hence their high cost, and severe human's health impact especially during their handling, could be considered as their serious drawbacks [22,23].

Therefore, in our study as a component responsible for double layer capacitance of the composite material we have used activated carbon. We have shown [21] that incorporation of the AC particles in the PPy – matrix sharply increases the electronic conductivity from  $\sim 200 \text{ F g}^{-1}$  for a neat PPy films to  $\sim 530 \text{ F g}^{-1}$  for PPy/AC composites containing  $\sim 55$  wt.% AC, results very similar to those elaborated in the literature for similar systems involving nanocomposites [4,24].

Our further research was concentrated on the synthesis of PPy and PPy/AC composite films with thicknesses ranging between 1.5 and 15  $\mu\text{m}$ , from non-aqueous, acetonitrile (ACN) solution containing  $0.1 \text{ mol dm}^{-3}$  Py and dispersed particles of activated carbon (AC). The concentration of the AC particles in the solution for electrochemical polymerization was  $30 \text{ g dm}^{-3}$ . The obtained composites were investigated by cyclic voltammetry and electrochemical impedance spectroscopy (EIS).

The increased conductivity noticed among the "neat" PPy films with higher thicknesses, and also at PPy/AC composites over that of the "pure" PPy film, has been discussed in relation with the developed microporosity of composite films and facilitated diffusion of doping anions in the films bulk.

Different equivalent electrical circuits were used to fit the experimental impedance data at anodic (0.2 V/SHE) and cathodic potentials ( $-0.6 \text{ V/SHE}$ ) at which the PPy as a pure polymer film and in the composites as well, are in the conducting and insulating states, respectively. As proposed [24], the electrical circuit model parameters for the best fitting suggested by the simulation software, describe the behavior of the porous structure, anion diffusion, and charge transfer effect.

## EXPERIMENTAL

High grade chemicals: pyrrole (Py, Merck), acetonitrile (ACN, Merck), sodium perchlorate (Aldrich), and activated carbon (AC, Merck) were used as received.

Specific area of activated carbon of  $\sim 540 \text{ m}^2 \text{ g}^{-1}$  was determined using spectrophotometric method ( $\lambda \approx 570 \text{ nm}$ ) and methylene blue as an absorbate.

Electrochemical synthesis of PPy and PPy/AC composite films were carried out by Chronoamperostat CEAMD 6 – Tacussel, in the three electrode cell containing  $0.1 \text{ mol dm}^{-3}$  Py and  $0.5 \text{ mol dm}^{-3}$   $\text{NaClO}_4$  (used as doping agent) dissolved in ACN, and dispersed AC particles ( $30 \text{ g dm}^{-3}$ ). The sedimentation of AC particles during the process of electrochemical synthesis was efficiently prevented by the agitation of the solution with purified nitrogen ( $\sim 120 \text{ bubbles min}^{-1}$ ).

Polymerization was performed with constant current of  $2.0 \text{ mA cm}^{-2}$  and the electrode potential of this process varied between 0.95 and 1.05 V/SHE. As shown previously [25] an anodic (polymerization) charge of  $0.36 \text{ C cm}^{-2}$  is necessary for deposition of 1  $\mu\text{m}$  PPy film. The polymerization process was performed within suitable time period necessary to obtain the previously assigned thicknesses of PPy in the "pure" polymer and in the composite films as well. The content of AC in the composites was determined by elemental analysis (EA).

A thermostated glass cell ( $25 \text{ }^\circ\text{C}$ ) with three electrode system, consisting of working, auxiliary and reference electrode was used during the synthesis and electrochemical characterization of the polymer and composite films. A platinum electrode with surface area,  $A = 1.7 \text{ cm}^2$ , was used as working electrode; platinum foil ( $\sim 20 \text{ cm}^2$ ) as an auxiliary electrode and saturated calomel electrode as reference electrode. All potentials were measured versus saturated calomel electrode (SCE) and are referred to the standard hydrogen electrode (SHE).

Polypyrrole (PPy) and the composite PPy/AC films were investigated using cyclic voltammetry and electrochemical impedance spectroscopy (EIS) at constant potentials in acetonitrile (ACN) solution containing  $0.5 \text{ mol dm}^{-3}$   $\text{NaClO}_4$ .

The cyclic voltammetry measurements (potentiostat connected to function generator, Institut für Physikalische Chemie und Elektrochemie, Heinrich Heine – Universität Düsseldorf) were performed in the potential window from 0.95 to  $-0.6 \text{ V/SHE}$ , and sweep rates ranging from 2 to  $30 \text{ mV s}^{-1}$ .

EIS measurements (frequency response analyzer TF 2000, Institut für Physikalische Chemie und Elektrochemie, Heinrich Heine – Universität Düsseldorf) were carried out in the frequency range from 100 kHz to 10 MHz at constant potential of 0.2 V/SHE, for the characterization of doped, and  $-0.6 \text{ V/SHE}$  for the undoped state of PPy and/or PPy/AC composite films; with a.c.

signal of 5 mV. The experimental results were fitted using software developed by Boukamp [26].

## RESULTS AND DISCUSSION

### Cyclic voltammetry

Electrochemical synthesis of PPy and PPy/AC composite films was performed at constant current density ( $2.0 \text{ mA cm}^{-2}$ ) from ACN electrolyte containing  $0.1 \text{ mol dm}^{-3}$  pyrrole,  $0.5 \text{ mol dm}^{-3}$   $\text{NaClO}_4$  and dispersed AC particles ( $30 \text{ g dm}^{-3}$ ). The thicknesses of PPy (from 0.5 to  $15 \text{ }\mu\text{m}$ ) as a “pure” polymer, and as a constituent in the composite films were regulated by parameter  $Q$  using the Eq. (1):

$$L_{\text{PPy}} = \frac{Q(M_{\text{Py}} + yM_{\text{ClO}_4^-})10^4}{(2+y)F\rho_{\text{PPy}}} \quad (\mu\text{m}) \quad (1)$$

where  $Q$  is the anodic charge of formation ( $\text{C cm}^{-2}$ ), and it was taken to be  $0.36 \text{ C cm}^{-2} \mu\text{m}^{-1}$  [25], while  $y$  is the doping level of the obtained PPy (usually 0.2–0.3), the density  $\rho_{\text{PPy}} = 1.51 \text{ g cm}^{-3}$  [21],  $M_{\text{Py}}$  is the molar mass of the pyrrole repeating unit and  $M_{\text{ClO}_4^-}$  the molar mass of the  $\text{ClO}_4^-$  doping anion, and  $F$  is the Faraday constant. As it was previously found the doping level of  $\text{ClO}_4^-$  in ACN solution was found to be 0.245 and 0.24 at the polymerization potentials of 0.95 and 1.05 V/SHE, respectively [25]. Regarding the thickness of polypyrrole (PPy) and composite (PPy/AC) films, as a first approx-

imation, the same density of both has been taken ( $\rho_{\text{PPy}} \approx \rho_{\text{PPy/AC}} \approx 1.51 \text{ g cm}^{-3}$ ).

Cyclic voltammograms of PPy and PPy/AC composite films in  $0.5 \text{ mol dm}^{-3}$   $\text{NaClO}_4$  obtained in potential range of  $-0.6$  to  $0.95$  V/SHE, and scan rates of 2 to  $30 \text{ mV s}^{-1}$  are presented in Figure 1. The linear dependences of capacitance current ( $j_c$ ) on sweep rates ( $dE/dt$ ) for different thicknesses (5, 10 and  $15 \text{ }\mu\text{m}$ ) of “neat” polymer and composite films are shown in Figure 2, while the corresponding voltammetric parameters are enclosed in Table 1.

Our observations of redox charge ( $q_{\text{red}}$ ) and capacitance ( $q_c$ ) enhancement for about 40% of PPy/AC – composites in respect to that of PPy-film confirm our previous observations [21] and literature data of similar systems [3,27]. Hence,  $q_{\text{red}}$  and  $q_c$  values from  $283 \text{ C g}^{-1}$  ( $216 \text{ F g}^{-1}$ ) for “pure” PPy-film increased to  $\sim 385 \text{ C g}^{-1}$  ( $\sim 318 \text{ F g}^{-1}$ ), for the PPy/AC composite films.  $q_{\text{red}}$  was calculated by the integration of an area under the voltammetric curves, Figure 1, and the values of the capacitance,  $q_c$ , were obtained according the Eq. (2) (as a slope of the linear  $j_c/(dE/dt)$  plots), Figure 2 [28,29]. The ratio  $q_c/q_{\text{red}}$  usually ranged about 0.8, for both, PPy and PPy/AC composite films, demonstrates a primary contribution of the capacitive component in the total current ( $j_{\text{total}} = j_c + j_f$ ).

$$C = j_c / d \left( \frac{\partial E}{\partial t} \right) \quad (2)$$

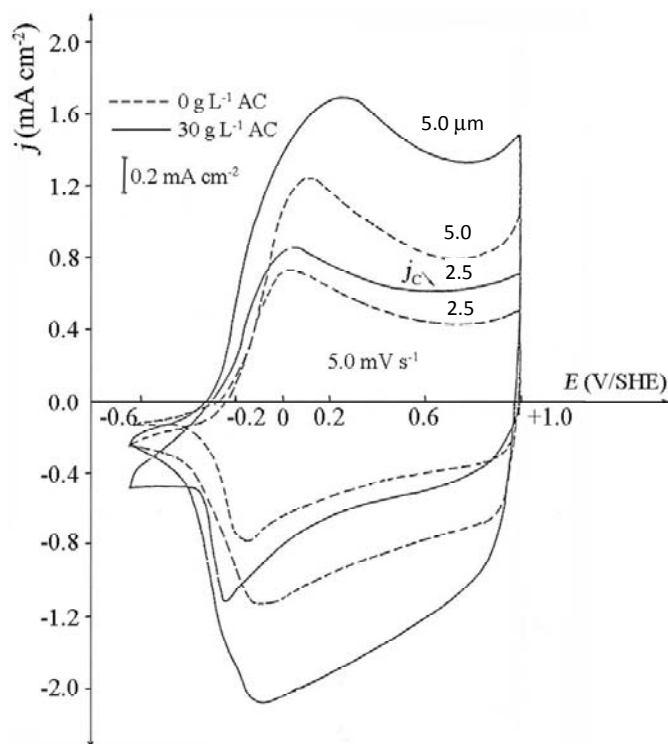


Figure 1. Voltammograms for PPy and PPy/AC – composite films synthesized from  $0.1 \text{ mol dm}^{-3}$  Py in  $0.5 \text{ mol dm}^{-3}$   $\text{NaClO}_4$ ;  $Q_{\text{pol.}} = 0.36 \text{ C cm}^{-2} \mu\text{m}^{-1}$ .

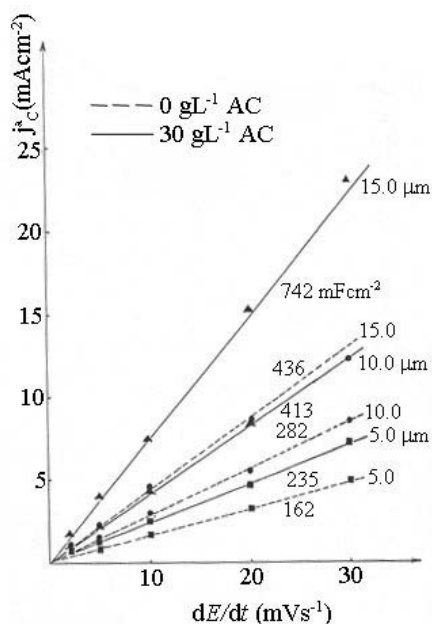


Figure 2.  $j_c/(dE/dt)$  dependences for composite PPy/AC films, with different thicknesses.

Table 1. Redox behavior of PPy and PPy/AC composite films obtained with dispersed particles of AC in the solution for electrochemical synthesis;  $C_{AC} = 30 \text{ g dm}^{-3}$ ;  $j_{pol.} = 2.0 \text{ mA cm}^{-2}$ ;  $Q_{pol.}$  – anodic charge necessary for polymerization of PPy of a given thickness;  $\tau_{pol.}$  – time of polymerization of PPy and PPy/AC composites;  $L_{PPy}$  – the thickness of the PPy film in the PPy/AC composite;  $L_{PPy/AC}$  – the thickness of the composite PPy/AC film, values given in the parenthesis; assuming  $\rho_{PPy} \approx \rho_{PPy/AC} = 1.51 \text{ g cm}^{-3}$ ;  $m_{PPy}^f$  – mass of the polypyrrole in the composite film;  $m_{PPy/AC}^f$  – mass of the composite film;  $m_{AC}^f$  – mass of activated carbon in the composite film;  $q_c$  – capacitance calculated from the voltammograms, by the relation:

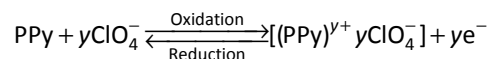
$$C = j_c / \left( \frac{dE}{dt} \right);$$

$q_{red}$  – redox capacitance, obtained by the graphical integration of the area under anodic and cathodic processes on the voltammograms

$Q_{pol.} / \text{C cm}^{-2}$	$\tau_{pol.} / \text{s}$	$L_{PPy}; L_{PPy/AC} / \mu\text{m}$	$m_{PPy}^f$	$m_{PPy/AC}^f$	$m_{AC}^f$	$q_{red} / \text{mC cm}^{-2}$		$q_c / \text{mF cm}^{-2}$	
						0	$30 \text{ g dm}^{-3} \text{ AC}$	0	$30 \text{ g dm}^{-3} \text{ AC}$
0.180	90	0.5 (~0.7)	0.075	0.105	0.030	22	–	16.8	–
0.540	270	1.5 (~2.43)	0.225	0.364	0.139	64.45	94.5	~58	62.5
0.900	450	2.5 (~4.55)	0.375	0.682	0.307	119	~142	92	108
1.800	900	5.0 (~8.85)	0.750	1.328	0.578	216	278	162	235
2.700	1350	7.5 (~13.43)	1.125	2.015	0.890	340	373	237	305
3.600	1800	10.0 (~18.13)	1.500	2.720	1.220	413	478	282	413
5.400	2700	15.0 (~27.07)	2.250	4.060	1.810	595	835	436	742

Significantly increased values of  $q_{red}$  and  $q_c$  for the composites are essentially attributed to the increased area of the solution / composite film interface and/or its capacitance similar to that shown for arrangements comprising electroconducting polymers and carbon based constituents [24,30,31]. Namely, in the case of the composite film mainly two processes take place: charging/discharging of the double layer AC particles/ /solution interface and the redox processes of the bulk PPy film [7,32,33]: it is known that the electrochemical behavior of PPy films is mainly based on their doping (oxidation)/undoping (reduction) processes, accom-

panied by the insertion and ejection of anions from a polymer film:



where  $\text{ClO}_4^-$  is a doping anion to compensate positive charges generated during oxidation processes, and  $y$  is the doping level.

The processes of doping (oxidation) of PPy films using the perchlorates are characteristic for the anodic potential range (0.9 – –0.2 V/SHE), while in the cathodic range (–0.2 – –0.6 V/SHE) PPy exists in its undoped (reduced) form.

The incorporated AC particles with their redox characteristics contribute to the redox behavior of the composite films. It is considered that the oxygen groups at the surface play the main role in the electrochemical behavior of activated carbon. The electronic conductivity of the activated carbon, mainly, does not depend on the potential, so as it was expected, their presence in the composite films provides a good conductivity, at

both oxidized and reduced state of polymer films. It was suggested that the synthesis of films with higher thicknesses and/or presence of AC particles increases the porosity of the composite films, which facilitate the  $\text{ClO}_4^-$  penetration in the films during doping, as well as their easier ejection during undoping processes [34].

The increased values of the capacitances of composite films in respect to those of “pure” PPy film, as well as, the linear  $q_{red}/L$  and  $q_c/L$  plots (correlation coefficient between 0.991 and 0.998), Figure 2 and Table 1, indicate a relatively homogenous distribution

of the AC particles irrespective to the thickness of the composite films.

### Electrochemical impedance spectroscopy (EIS) study

The study performed by electrochemical impedance spectroscopy (EIS) confirms the electrochemical behavior of PPy and PPy/AC composite films shown in Figures 1 and 2, and Table 1.

Bode plots ( $\log Z - \log f$ , and  $\varphi - \log f$ ) of PPy/AC composite films with doped state of PPy ( $E = 0.2$  V/SHE), are presented in Figure 3.

The impedance behavior of composite films indicates the existence of two regions:

The first one, between 100 kHz and  $\sim 10$  Hz, with a small and almost constant values of the impedance,  $Z$ , and the values of the phase angle,  $\varphi$ , between 0 and  $-60^\circ$ , is mainly attributed to the ohmic behavior of the electrolyte between the working and the reference electrode.

The second frequency range,  $f \leq 10$  Hz, where  $Z$  and  $\varphi$  linearly increase in accordance with a “finite diffusion model” of Ho *et al.* [25,32], characterized by the existence of the diffusion controlled doping/undoping processes in the bulk of the composite films [32,33].

The impedance characteristics of the PPy/AC systems are summarized in Table 2, where  $R_{el}$  – resistance of the electrolyte ( $Z' \approx R_{el} = \sim 13 \Omega \text{ cm}^2$ , determined at  $f \rightarrow \infty$ ),  $R_L$  – limiting resistivity of the films,  $R_{total}$  – total resistance ( $R_{total} = R_{el} + R_L$ ), extrapolated at very low frequencies ( $Z' \approx R_{total}$ , at  $f \rightarrow 0$ ),  $C_L$  – limiting capacitance of the film, and  $D$  – diffusion constant of doping anions.

The values of the limiting capacitance,  $C_L$ , listed in the Table 2, are calculated from the linear plots:  $-Z''/(1/\omega)$ , shown in Figure 4, according the Eq. (3):

$$1/C_L = d(-Z'')/d(1/\omega) \quad (3)$$

where  $\omega$  is an angular frequency ( $\omega = 2\pi f$ ).

The linear dependences of  $C_L$  of polymer and composite films on their thicknesses are shown in Figure 5. Increasing values of the limiting capacitance,  $C_L$ , of the PPy/AC composite films compared to that of a “pure” PPy films, Figure 5, is in accordance to the previously calculated values of  $q_c$ . Namely, limiting capacitance ( $C_L$ ) of the composite films, takes values of  $\sim 260 \text{ F g}^{-1}$  ( $\sim 73 \text{ A h kg}^{-1}$ ) compared to  $\sim 180 \text{ F g}^{-1}$  ( $\sim 50 \text{ A h kg}^{-1}$ ) for the PPy film, which is very close to those of similar systems [35].

The diffusion coefficient,  $D$ , of the doping anions ( $\text{ClO}_4^-$ ), for PPy/AC composite films, is calculated by equation:  $D = L^2/3R_L C_L$ , according to the diffusion model of Ho *et al.* [32]. It is obvious that for relatively small thicknesses, the diffusion coefficient takes values in the order of magnitude of  $10^{-9} \text{ cm}^2 \text{ s}^{-1}$  (increasing with the thickness of the composite films, Table 2). This phenomenon is most probably result of the facilitated transport of the doping anions in the bulk of the composites, that could be ascribed, as it was shown in the literature, to the increased amount of both, PPy and AC particles in the films [19,36]. The values of the diffusion coefficients which depend on the thickness and morphology of the film, the synthesis condition, as well as the nature of the doping anion, are in accordance to the literature data [19,25,33,36]. Thus, Malviya *et al.*

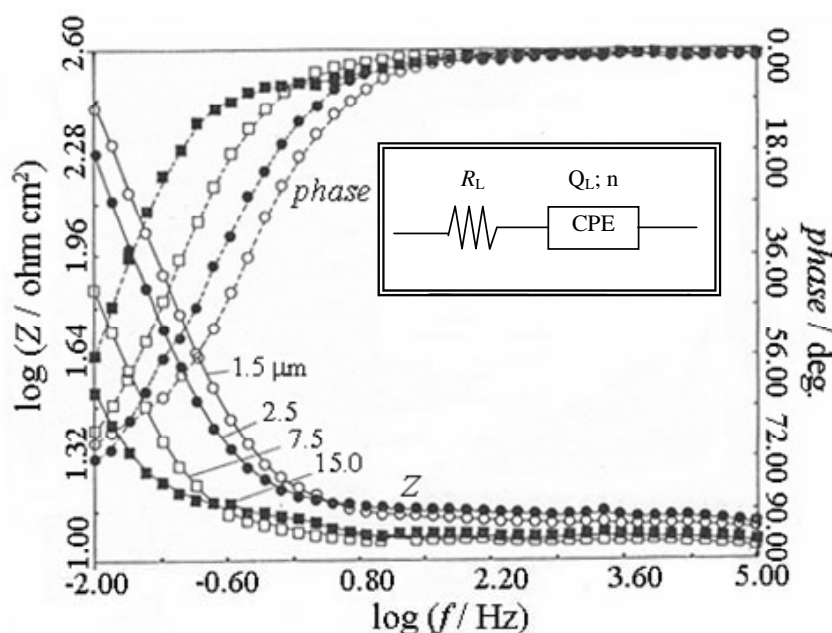
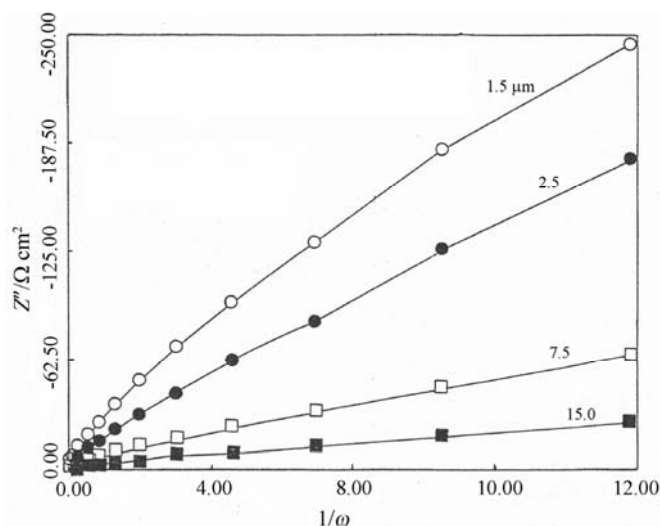


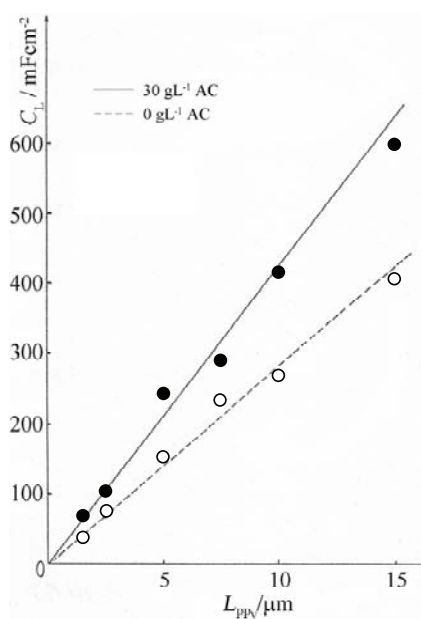
Figure 3. Bode plots ( $\log Z - \log f$ , and  $\varphi - \log f$ ) of PPy/AC composite films ( $30 \text{ g dm}^{-3}$  AC) with different thicknesses, in doped ( $E = 0.2$  V/SHE) state of PPy in the  $0.5 \text{ mol dm}^{-3}$   $\text{NaClO}_4/\text{ACN}$  solution.

Table 2. Impedance characteristics of PPy/AC composite films in doped (oxidized) state of PPy;  $C_{AC} = 30 \text{ g dm}^{-3}$ ;  $E = 0.2 \text{ V/SHE}$ 

$L_{PPy} / \mu\text{m}$ ( $m_{PPy}^f / \text{mg cm}^{-2}$ )	$R_{el} / \Omega \text{ cm}^2$	$R_L / \Omega \text{ cm}^2$	$R_{total} / \Omega \text{ cm}^2$	$C_L / \text{mF cm}^{-2}$	$D \times 10^8 / \text{cm}^2 \text{ s}^{-1}$
1.5 (0.225)	$13 \pm 0.5$	87	$\sim 100$	$\sim 68$	0.127
2.5 (0.375)		49	64	107	0.397
5.0 (0.750)		16.5	30	244	2.07
7.5 (1.125)		16.0	$\sim 28$	360	3.26
10.0 (1.5)		12.0	$\sim 27$	405	6.86
15.0 (2.25)		$\sim 5.5$	$\sim 22$	587	17

Figure 4.  $Z'' - 1/\omega$  plots for PPy/AC composite films ( $30 \text{ g dm}^{-3}$ ) with different thicknesses, in the  $0.5 \text{ mol dm}^{-3} \text{ NaClO}_4/\text{ACN}$  solution for the doped ( $E = 0.2 \text{ V/SHE}$ ) state of PPy.

found that the diffusion coefficient of a less voluminous chlorine anion in PPy system is of the order of magnitude of  $10^{-7} \text{ cm}^2 \text{ s}^{-1}$  [36].

Figure 5.  $C_L/L_{PPy}$  plots (calculated from the  $-Z''/(1/\omega)$ ) for PPy and composite PPy/AC films in the doped ( $E = 0.2 \text{ V/SHE}$ ) state of PPy, in the solution of  $0.5 \text{ mol dm}^{-3} \text{ NaClO}_4$  (ACN).

Nyquist ( $-Z''$  vs.  $Z'$ ) plots of PPy and composite PPy/AC films, for the conducting state of polymer component, are presented in Figure 6a and b.

The impedance behavior of “neat” PPy and/or PPy/AC composite films, for the best fit of the experimentally obtained data, in the conducting state of PPy ( $E = 0.2 \text{ V/SHE}$ ), as suggested by the simulation software developed by Boukamp [26], can be described by a simple RQ equivalent electrical circuit (EEC), presented in Figure 7a [31,37]. On the other hand, it appears that EEC presented in the Figure 7b [19,31,37] gives significantly better agreement to the  $-Z''/Z'$  plots, Figure 6a and b. Such a behavior has been observed mainly for composite films with the thicknesses higher than  $2.5 \mu\text{m}$ .

The best fitting parameters of R(QR)Q equivalent electrical circuit (Figure 7b) for PPy and composite PPy/AC films, as proposed by the software, are given in Table 3.  $R_{el}$  denotes the ohmic resistance of the electrolyte,  $R_{ct}$  is proportional to the charge transfer resistance, the element  $Q_1$  (with the exponential coefficient  $n_1$ ), known as constant phase element (CPE), correspond to the double layer capacitance,  $C_{dl}$  ( $C_{dl} = Q_1^{1/n}$ ). For  $L_{PPy} \geq 2.5 \mu\text{m}$  the coefficients  $n_1$  takes similar values for both, PPy and PPy/AC films, indicating diffusion or mixed (ohmic-diffusion) control at the film/solution

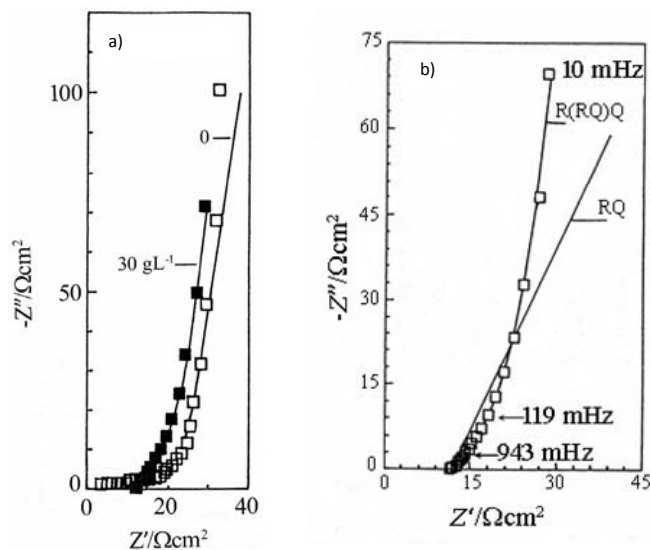


Figure 6. Nyquist plots for PPY (a) and composite PPY/AC film (a and b),  $L_{PPy} = 5 \mu m$ , in the oxidized (doped) state of PPY ( $E = 0.2 V/SHE$ ) in  $0.5 mol dm^{-3} NaClO_4/ACN$  solution for the RQ and R(QR)Q EEC; experimentally obtained values of “neat” PPY: (-□-) and PPY/AC composites: (-■-); simulation: (—).

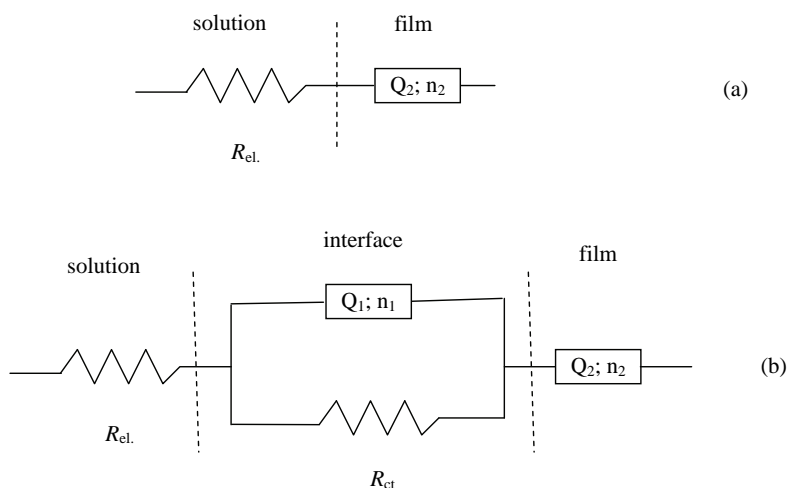


Figure 7. Electrical equivalent circuit for doped ( $E = 0.2 V/SHE$ ) state of PPY ( $L_{PPy} = 5 \mu m$ ) in the PPY/AC composite film.

Table 3. The best fitting impedance parameters of R(QR)Q equivalent electrical circuit (Figure 7b) for PPY (values given in the parenthesis) and composite PPY/AC films,  $C_{AC} = 30 g dm^{-3}$ ,  $E = 0.2 V/SHE$

$L_{PPy} / \mu m$	$R_{el.}$	$R_{ct}$	$Q_1/\Omega^{-1} s^n cm^{-2}$	$n_1$	$Q_2/\Omega^{-1} s^n cm^{-2}$	$n_2$
	$\Omega cm^2$					
0.5	—	—	—	—	—	—
	(4.1)	(46.0)	$(7.23 \cdot 10^{-4})$	(0.53)	$(1.14 \cdot 10^{-2})$	(0.907)
1.5	12.0	4.4	0.224	0.127	$3.3 \cdot 10^{-2}$	0.783
	(3.0)	(36.0)	$(5.22 \cdot 10^{-4})$	(0.485)	$(3.27 \cdot 10^{-2})$	(0.917)
2.5	12.8	$4.9 \cdot 10^{18}$	0.36	0.120	$5.54 \cdot 10^{-2}$	0.82
	(3.2)	(131.0)	$(5.94 \cdot 10^{-5})$	(0.735)	$(2.25 \cdot 10^{-2})$	(0.735)
5.0	~12	23.5	0.123	0.517	0.235	0.977
	(~0)	(~33)	$(1.11 \cdot 10^{-2})$	(0.226)	(0.119)	(0.921)
10.0	14.1	527	0.533	0.511	0.262	0.913
	(11.6)	(~9)	$(1.445 \cdot 10^{-2})$	(0.525)	(0.207)	(0.88)
15.0	11.3	4.31	0.082	0.572	0.416	0.879
	(-)	(-)	(-)	(-)	(-)	(-)

interface [24,35]. The very slow processes in the bulk of the composite films are presented by a phase element  $Q_2$  (with the exponent  $n_2$ ), proportional to the limiting capacitance,  $C_L$ . The coefficient  $n_2$  with a substantially higher values clearly shows a relatively close behavior to that of an ideal capacitor ( $n = 1$ ). The difference in the values of the limiting capacitance  $Q_2$  ( $28.4 \text{ mF cm}^{-2} \mu\text{m}^{-1}$ ), of PPy/AC composites, calculated by regression analysis ( $Q_2/L$ ) of data in Table 3, and the limiting capacitance,  $C_L$  ( $39.4 \text{ mF cm}^{-2} \mu\text{m}^{-1}$ ), obtained using the

$-Z''/(1/\omega)$  dependences, is most probably result of the different EECs considered. Namely, the simple RQ circuit, Fig. 7a, was applied during determination of  $C_L$ , while  $Q_2$  values are obtained with the R(QR)Q EEC, more consistent with the experimentally obtained data (Fig. 7b).

Bode and Nyquist plots in Figures 8 and 9, respectively, concern the features of PPy film ( $5 \mu\text{m}$ ) in doped ( $E = 0.2 \text{ V/SHE}$ ) and undoped ( $E = -0.6 \text{ V/SHE}$ ) states, indicating some qualitative and quantitative differences

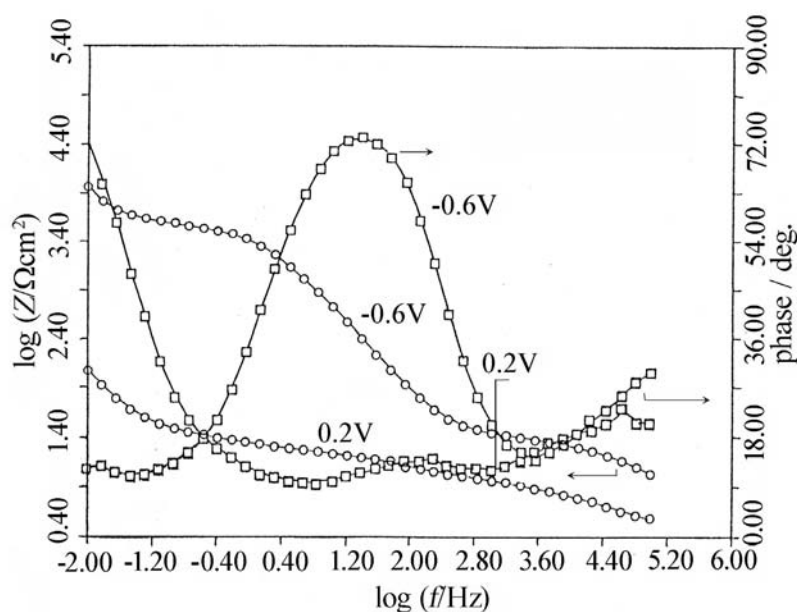


Figure 8. Bode plots ( $\log Z - \log f$ , and  $\phi - \log f$ ) for PPy film ( $5 \mu\text{m}$ ) in doped ( $E = 0.2 \text{ V/SHE}$ ) and undoped ( $E = -0.6 \text{ V/SHE}$ ) states, in  $0.5 \text{ mol dm}^{-3} \text{ NaClO}_4/\text{ACN}$  solution.

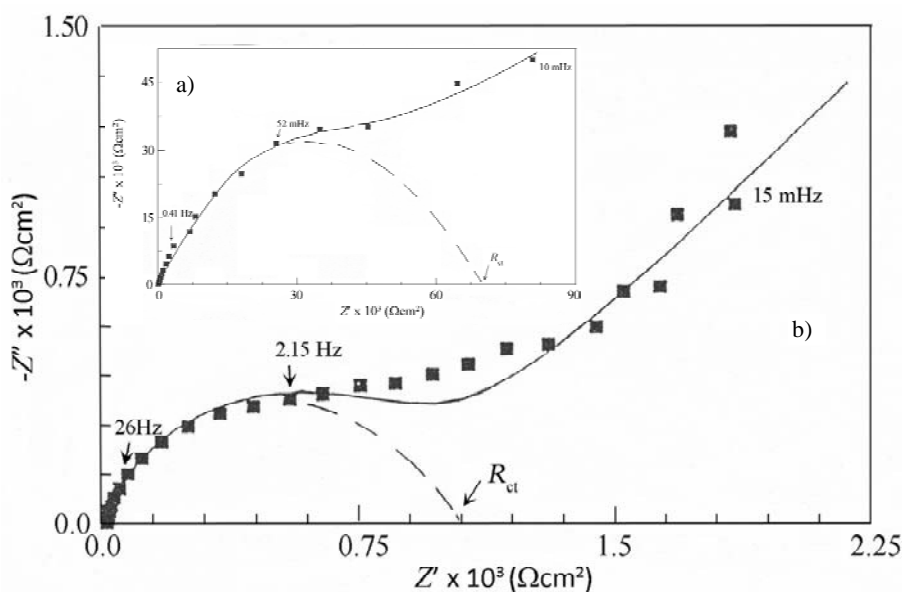


Figure 9. Nyquist plot ( $-Z''/Z'$ ) for a) PPy film and b) composite PPy/AC film ( $30 \text{ g dm}^{-3} \text{ AC}$ ),  $L_{\text{PPy}} = 7.5 \mu\text{m}$ , in the undoped ( $E = -0.6 \text{ V/SHE}$ ) state of PPy, in  $0.5 \text{ mol dm}^{-3} \text{ NaClO}_4/\text{ACN}$  solution, for the best fitting R(QR)Q (a) and R[Q(RW)] (b) EEC; experimentally obtained values of "neat" PPy and PPy/AC composites: (■-); simulation: (—).



in the impedance behavior of PPy and composite PPy/AC films in both, doped (conducting) and undoped (insulating) state of PPy.

When undoped state of PPy, “neat” and as a part of composite PPy/AC films is concerned, the dominant semicircles in  $-Z''/Z'$  plots, Figure 9, attributed to the charge transfer processes at the polymer/solution interface, and the linear part of these dependences, at very low frequencies, characteristic for diffusion controlled processes, Warburg impedance [35], can be expressed by the EECs in Figure 10a and b. Namely, the simpler EEC, Figure 10a, has been used for fitting the data obtained for the films with lower thicknesses, while for the systems with higher thicknesses, a more complex EEC, Figure 10b, should be applied.

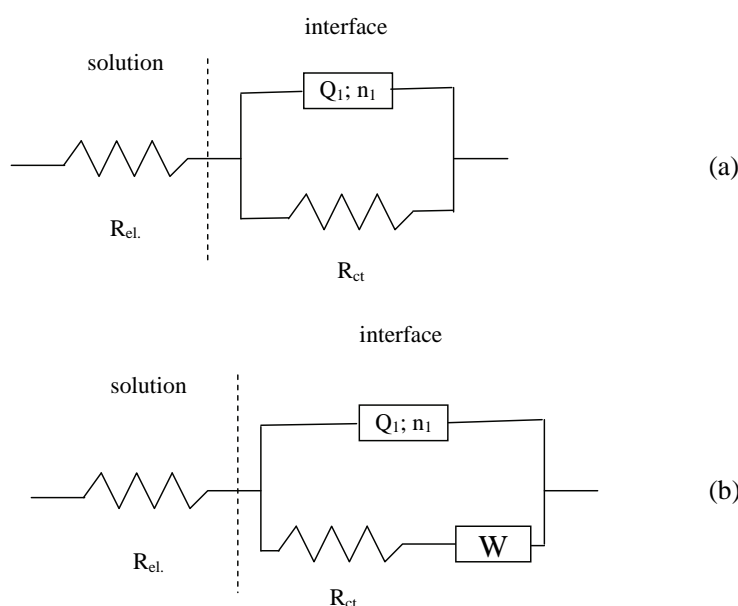


Figure 10. Equivalent electrical circuits  $R(QR)$  for PPy film (a) and  $R[Q(RQ)]$  for PPy/AC composite film (b), in undoped ( $E = -0.6$  V/SHE) state of PPy.

The ohmic charge transfer resistance,  $R_{ct}$ , depends on both, the film thickness, and the quantity of AC particles in the composite film. The presence of the AC particles in composite film reduces the volume resistivity,  $\rho$ , for about two orders of magnitude in respect to that of the PPy-film. Thus,  $\rho = 7 \times 10^4 / 7.5 \times 10^{-4} = 10^8 \Omega \text{ cm}$  (the  $R_{ct}$  value is  $\sim 70 \text{ k}\Omega \text{ cm}^2$ ) for PPy film (Figure 9a), while  $\rho$  of the PPy/AC composite film, with the same thickness (Figure 9b), takes value of  $1000 / 7.5 \times 10^{-4} = 1.3 \times 10^6 \Omega \text{ cm}$  ( $R_{ct} \approx 1 \text{ k}\Omega \text{ cm}^2$ ). Such a behavior is most likely related to an increased conductivity and microporosity of these films. Two types of conductivities are characteristic for PPy/AC composites: ionic and electronic. Composites comprise two independent components: a polymer responsible for ionic conductivity, while AC with its physical and chemical properties provides the electronic conductivity of these systems,

which mainly depends on the concentration of AC particles in the composites, and is almost independent on the given potential.

## CONCLUSIONS

Polypyrrole (PPy) and composites based on polypyrrole/activated carbon (PPy/AC), with the thickness of PPy in both, the “neat” and the composite films ranged 1.5 and 15  $\mu\text{m}$ , were synthesized electrochemically, from non-aqueous, acetonitrile (ACN) solution containing Py ( $0.1 \text{ mol dm}^{-3}$ ) and constant concentration of activated carbon (AC) ( $30 \text{ g dm}^{-3}$ ). The obtained composites were investigated by cyclic voltammetry and electrochemical impedance spectroscopy (EIS).

It was shown that the best fitting EEC, for PPy and/or PPy/AC composite films in their conducting state is the  $R(QR)Q$  equivalent electrical circuit, and  $R[Q(RW)]$  equivalent electrical circuit for the insulating state.

The charge transfer resistance ( $R_{ct}$ ) depends on both, the thickness of the films, as well as, the presence of the AC in the composites. A higher quantity of AC in the PPy/AC composites decreases the volume resistivity for two orders of magnitude in respect to a “pure” PPy films, in both, conducting and insulating states ( $\rho = 1.3 \times 10^6 \Omega \text{ cm}$  for the composite PPy/AC film,  $L = 7.5 \mu\text{m}$ , and  $\rho \approx 10^8 \Omega \text{ cm}$  for the PPy film with the same thickness).

Based on the previously presented results of the PPy/AC electroconducting composites comprising two electrochemically active components, such as DLC

(double layer capacitors)–active carbon and redox properties of PPy, can be effectively used in supercapacitors and/or batteries.

## REFERENCES

- [1] B.E. Conway, W.G. Pell, Double layer and pseudocapacitance types of electrochemical capacitor and their applications to the development of hybrid devices, *J. Solid State Electrochem.* **7** (2003) 637–644.
- [2] E.D. Laird, M.A. Hood, C.Y. Li, in: Y. Gogotsi, V. Presser (Eds.), *Carbon nanomaterials* CRC Press, Taylor & Francis Group, Boca Raton, FL, 2006, pp. 135–187.
- [3] J-H. Kim, Y-S. Lee, A.K. Sharma, C.G. Liu, Polypyrrole/carbon composite electrode for high-power electrochemical capacitors, *Electrochim. Acta* **52** (2006) 1727–1732.
- [4] A. Imani, G. Farzi, A. Ltaief, Facile synthesis and characterization of polypyrrole-multiwalled carbon nanotubes by in situ oxidative polymerization, *Int. Nano Lett.* **52** (2013) 1–8.
- [5] S. Paul, J-H. Kim, D-W. Kim, Cycling performance of supercapacitors assembled with polypyrrole/multiwalled carbon nanotube/conductive carbon composite electrodes, *J. Electrochem. Sci. Techn.* **2** (2011) 91–96.
- [6] P. Simon, Y. Gogotsi, Materials for electrochemical capacitors, *Nat. Mater.* **7** (2008) 845–854.
- [7] S.M. Jovanovic, R. Stankovic, V. Laninovic, G. Nestorovic, M. Popovic, B. Vidic, O. Pavlovic, N. Krstajic, B. Grgur, M. Vojnovic, S. Stankovic, Synthesis and electrochemical properties of polypyrrole, polyaniline and poly-3-methyl thiophene, *Hem. Ind.* **54** (2000) 417–427.
- [8] M. Natalie, R.J. Mortimer, R.J. Mortimer, *New Electrochromic Materials*, *Sci. Prog.* **85** (2002) 243–262.
- [9] J. Zhang, L-B. Kong, H. Li, Y-Ch. Luo, L. Kang, Synthesis of polypyrrole film by pulse galvanostatic method and its application as supercapacitor electrode materials, *J. Mater. Sci.* **45** (2010) 1947–1954.
- [10] C. Mao, A. Zhu, Q. Wu, X. Chen, J. Kim, J. Shen, New biocompatible polypyrrole- based films with good blood compatibility and high electrical conductivity, *Colloids Surfaces, B* **67** (2008) 41–45.
- [11] D. Beattie, K.H. Wong, C. Williams, L.A. Poole-Warren, T.P. Davis, C. Barner-Kowollik, M.H. Stenzel, Honeycomb-structured porous films from polypyrrole-containing block copolymers prepared *via* RAFT polymerization as a scaffold for cell growth, *Biomacromolecules* **7** (2006) 1072–1082.
- [12] J. Zhang, S. Wang, M. Xu, Y. Wang, H. Xia, S. Zhang, X. Guo, S. Wu, Polypyrrole-coated SnO<sub>2</sub> hollow spheres and their application for ammonia sensor. *J. Phys. Chem., C* **113** (2009) 1662–1665.
- [13] H.K. Song, G.T.R. Palmore, Redox-active polypyrrole: toward polymer-based batteries, *Adv. Mater.* **18** (2006) 1764–1768.
- [14] Q. Ameer, S.B. Adeloju, Polypyrrole-based electronic noses for environmental and industrial analysis, *Sens. Actuators, B* **106** (2005) 541–552.
- [15] N.V. Krstajić, B.N. Grgur, S.M. Jovanović, M.V. Vojnović, Corrosion protection of mild steel by polypyrrole coatings in acid sulfate solutions. *Electrochim. Acta* **42** (1997) 1685–1691.
- [16] L. Koene, W.J. Hamer, J.H. De Wit, Electrochemical behavior of poly(pyrrole) coatings on steel, *J. Appl. Electrochem.* **36** (2006) 545–556.
- [17] H. Shokry, Corrosion protection of mild steel electrode by electrochemical polymerization of acrylamide, *Chem. Met. Alloys* **2** (2009) 202–210.
- [18] R. Kotz, M. Carlen, Principles and applications of electrochemical capacitors, *Electrochim. Acta* **45** (2000) 2483–2498.
- [19] E. Kalaycioglu, L. Toppare, T. Grchev, M. Cvetkovska, Y. Yagci, Impedance characteristics of conducting polypyrrole-poly(ethylvinylether) graft films, *Turk. J. Chem.* **23** (1999) 1–7.
- [20] M.Cvetkovska, T. Grchev, T. Obradovic, Electroconductive polymer composite: Fibrous carrier-polypyrrole, *J. Appl. Polym. Sci.* **60** (1996) 2049–2058.
- [21] A. Porjazoska Kujundziski, D. Chamovska, M. Cvetkovska and T. Grchev, Electrochemical Study of Electroconducting Composite Material–Polypyrrole/Activated Carbon, *Int. J. Electrochem. Sci.* **7** (2012) 4099–4113.
- [22] G. Tejral, N.R. Panyala, J. Havel, Carbon nanotubes: toxicological impact on human health and environment, *J. Appl. Biomed.* **7** (2009) 1–13.
- [23] A. Helland, P. Wick, A. Koehler, K. Schmid, C. Som, Reviewing the environmental and human health knowledge base of carbon nanotubes, *Environ. Health Perspect.* **115** (2007) 1125–1131.
- [24] B. Veeraraghavan, J. Paul, B. Haran, B. Popov, Study of polypyrrole graphite composite as anode material for secondary lithium-ion batteries, *J. Power Sources* **109** (2002) 377–387.
- [25] T. Grcev, M. Cvetkovska, Z. Sekovska, Voltammetric study of the redox processes of polypyrrole films, *J. Serb. Chem. Soc.* **58** (1993) 781–790.
- [26] B.A. Boukamp, A Nonlinear Least Squares Fit procedure for analysis of immittance data of electrochemical systems, *Solid State Ionics* **20** (1986) 31–44.
- [27] V. Khomenko, E. Frackowiak, F. Béguin, Determination of the specific capacitance of conducting polymer/nanotubes composite electrodes using different cell configurations, *Electrochim. Acta* **50** (2005) 2499–2506.
- [28] J.W. Schultze, A. Thyssen, The kinetics of electropolymerization, *Synth. Met.* **43** (1991) 2825–2830.
- [29] T.F. Otero, E. Angulo, Comparative kinetic studies of polypyrrole electrogeneration from acetonitrile solutions, *J. Appl. Electrochem.* **22** (1992) 369–375.
- [30] T. Grchev, M. Cvetkovska, T. Obradovic, Redox properties of an electrochemically activated (oxidized) carbon fibre electrode, *J. Serb. Chem. Soc.* **62** (1997) 157–164.
- [31] M. Ates, Review study of electrochemical impedance spectroscopy and equivalent electrical circuits of conducting polymers on carbon surfaces, *Prog. Org. Coat.* **71** (2011) 1–10.

- [32] C. Ho, I.D. Raistrick, R.A. Huggins, Application of A-C Techniques to the Study of Lithium Diffusion in Tungsten Trioxide Thin Films, *J. Electrochem. Soc.* **127** (1980) 343–350.
- [33] J. Mostany, B.R. Scharifker, Impedance spectroscopy of undoped, doped and overoxidized polypyrrole films, *Synth. Met.* **87** (1997) 179–185.
- [34] E. Frackowiak, F. Beguin, Carbon materials for the electrochemical storage of energy in capacitors, *Carbon* **39** (2001) 937–950.
- [35] P.A. Basnayaka, M.K. Ram, L. Stefanakos, A. Kumar, Graphene/polypyrrole nanocomposite as electrochemical supercapacitor electrode: electrochemical impedance studies, *Graphene* **2** (2013) 81–87.
- [36] M. Malviya, J.P. Singh, B. Lal, R.N. Singh, Transport behavior of  $\text{Cl}^-$  in composite films of polypyrrole and  $\text{CoFe}_2\text{O}_4$  obtained for oxygen reduction, *New J. Mat. Electrochem. Sys.* **8** (2005) 223–228.
- [37] M.M. Lohrengel, O. Genz, Mechanism of the redox process of conducting polymers, *Ionics* **4** (1995) 304–310.

## IZVOD

### KAPACITIVNA SVOJSTVA KOMPOZITNIH FILMOVA POLIPIROL/AKTIVNI UGALJ

Aleksandra Porjazoska Kujundžiski<sup>1</sup>, Dragica Čamovska<sup>2</sup>, Toma Grčev<sup>2</sup>

<sup>1</sup>*International Balkan University, Faculty of engineering, Macedonia*

<sup>2</sup>*Faculty of Technology and Metallurgy, Sts. Cyril & Methodius University, Skopje, Macedonia*

(Naučni rad)

Elektrohemijska sinteza polipirola (PPy) i kompozitnih filmova polipirol/aktivni ugalj (PPy/AU) različitih debljina od 0,5 do 15  $\mu\text{m}$ , ostvarena je u uslovima konstante količine naelektrisanja, iz rastvora acetonitrila koji je sadržavao 0,5  $\text{mol dm}^{-3}$   $\text{NaClO}_4$ ; 0,1  $\text{mol dm}^{-3}$  pirola (Py) i dispergovane čestice aktivnog uglja (30  $\text{g dm}^{-3}$ ). Elektrohemijske karakteristike PPy i PPy/AU kompozitnih filmova određene su pomoću ciklične voltametrije i spektroskopije elektrohemijske impedancije. Linearne zavisnosti kapacitivnosti ( $q_c$ ), redoks kapacitivnosti ( $q_{red}$ ) i granične kapacitivnosti ( $C_L$ ) od debljine polipirolnih i kompozitnih filmova ( $L$ ) ukazuju na homogenu distribuciju inkorporiranih čestica aktivnog uglja u kompozitne filmove. Primećeno je znatno povećanje  $q_c$ ,  $q_{red}$ , i  $C_L$  vrednosti za kompozitne filmove ( $\sim 40\pm 5\%$ ) u odnosu na iste veličine "čistog" PPy filma. Uočeno je da kompozitni filmovi u neprovodnom stanju imaju za oko dva reda veličine manje vrednosti za specifičnu otpornost,  $\rho = 1,3 \times 10^6 \Omega \text{ cm}$ , (za  $L = 7,5 \mu\text{m}$ ) u poređenju sa PPy filmovima iste debljine,  $\rho \approx 10^8 \Omega \text{ cm}$ .

*Ključne reči:* Elektroprovodni polimeri • kompoziti • Ciklična voltametrija • Spektroskopija elektrohemijske impedancije • Električna ekvivalentna kola